Available online at www.sciencedirect.com
ScienceDirect
Journal of Sound and Vibration 307 (2007) 894–905
JOURNAL OF SOUND AND VIBRATION
www.elsevier.com/locate/jsvi

Sudden lateral asymmetry and torsional oscillations of section models of suspension bridges

R.H. Plaut[a,*], F.M. Davis[b]

[a]Department of Civil and Environmental Engineering, Virginia Polytechnic Institute and State University, Blacksburg, VA 24061, USA
[b]Department of Engineering Science and Mechanics, Virginia Polytechnic Institute and State University, Blacksburg, VA 24061, USA

Received 13 June 2006; received in revised form 21 February 2007; accepted 24 July 2007
Available online 29 August 2007

Abstract

Cable-supported bridges typically exhibit minimal torsional motion under traffic and wind loads. If symmetry of the bridge about the deck's centerline is suddenly lost, such as by the failure of one or more cables or hangers (suspenders), torsional motion of the deck may grow and angles of twist may become large. The initiation of the disastrous torsional oscillations of the original Tacoma Narrows Bridge involved a sudden lateral asymmetry due to loosening of a cable band at midspan. The effects of these types of events on two-degree-of-freedom and four-degree-of-freedom section models of suspension bridges are analyzed. Vertical and rotational motions of the deck, along with vertical motions of the cables, are considered. A harmonic vertical force and an aerodynamic moment proportional to angular velocity are applied to the deck. Resistance is provided by translational and rotational springs and dashpots. Flutter instability and large oscillations occur under the aerodynamic moment, which provides "negative damping." In order to model the occurrence of limit cycles, nonlinear damping of the van der Pol type is included in one case, and nonlinear stiffness of the hangers in others. The frequencies of the limit cycles are compared to the natural frequencies of the system.

1. Introduction

The original Tacoma Narrows Bridge exhibited significant vertical oscillations after it opened on July 1, 1940. On November 7, 1940, the band restraining one of the main suspension cables at midspan loosened, and the cable began to slip back and forth through the band [1]. This created an asymmetrical condition with respect to the centerline of the bridge, and initiated torsional oscillations of the deck in addition to vertical motion. The torsional oscillations caused the bridge to collapse about an hour later. Another condition that could cause sudden lateral asymmetry is the loss of one or more hangers on one side of a bridge. The effect of these types of events is considered here through the dynamic response of some simple section models.

Papers analyzing coupled vertical–torsional oscillations of section models of the original Tacoma Narrows Bridge will be described, starting with two-degree-of-freedom models. In those, the ends of the horizontal rigid bar representing the deck cross section are suspended by vertical springs representing the effect of the main

*Corresponding author. Tel.: +1 540 231 6072; fax: +1 540 231 7532.
E-mail address: rplaut@vt.edu (R.H. Plaut).

0022-460X/$ - see front matter © 2007 Elsevier Ltd. All rights reserved.
doi:10.1016/j.jsv.2007.07.036

suspension cables and the vertical hangers (suspenders) from those cables to the deck. The coordinates are the vertical motion of the bar's center of mass and the rotational (torsional) motion about the center of mass.

Rocard [2] considered small displacements. The center of gravity was not always at the geometrical center of the model, and the springs were allowed to have unequal stiffnesses. The wind was assumed to apply a moment and a vertical force, both of which were linear functions of the rotation and the vertical velocity. For this model, the critical wind speed was determined.

Lazer and McKenna [3] assumed that the springs do not resist compression, and resist extension with the usual linear relationship. Large rotations (torsional motions) of the bar were included in the equations of motion, along with viscous damping of the vertical and rotational motions. Translational and rotational springs represented the resistance of the rest of the deck to motion. A vertical force and a pitching moment that varied harmonically in time were applied at the center of mass. The nonlinearities due to large rotations and the nonlinear springs allowed multiple steady-state solutions to exist. The authors felt that nonlinear (taut/slack) behavior of the hangers (i.e., alternate slackening and tightening) was an important factor in the failure of the original Tacoma Narrows Bridge. This claim stirred up a lively controversy (e.g., Refs. [4–6]).

Jacover and McKenna [7] presented additional results for the same model. McKenna [8] deleted the restoring force and moment due to the deck, and vertical excitation. Various initial conditions were applied, leading to several types of response. Doole and Hogan [9] applied techniques of nonlinear dynamics to investigate possible periodic motions. They used the Lazer–McKenna model except that the bilinear spring function was replaced by a smooth function.

McKenna and Ó Tuama [10] also utilized a smooth version of the nonlinear spring force. In their computations, no torsional forcing was applied, and the vertical force had a high frequency. Resistance from the deck was not included. It was shown that a torsional perturbation could lead to large torsional oscillations. McKenna and Moore [11] included torsional excitation and compared results for the bilinear spring with those for the smoothed spring function. Also, periodic solutions for the smoothed system were determined.

Two related papers using a four-degree-of-freedom model are Sepe and Augusti [12] and Sepe et al. [13]. In addition to the vertical and rotational motions of the suspended bar, vertical motions of point masses representing the suspension cables were included. These masses were suspended by vertical springs, and each end of the bar was suspended from the corresponding mass by a vertical spring that did not resist compression. Vertical and rotational springs were attached to the center of mass of the bar, as in the Lazer–McKenna model, and viscous damping was active for all four displacements. In Ref. [13], harmonically varying vertical forces were applied to the point masses (with a relative phase lag) and to the center of mass of the deck, along with a moment applied to the deck with the same frequency as the forces. Small displacements were assumed. The bilinear lower springs allowed multiple steady-state solutions to be exhibited.

Most of the previous studies have considered symmetric section models of bridges. In this paper, models that are asymmetric, or suddenly become asymmetric, are analyzed. A two-degree-of-freedom section model is formulated in Section 2, and results are presented in Section 3. Then the formulation and results for a four-degree-of-freedom model are given in Sections 4 and 5, respectively. Section 6 contains concluding remarks.

2. Formulation for two-degree-of-freedom model

The two-degree-of-freedom model considered here is shown in Fig. 1. Fig. 1(a) depicts the system in its equilibrium configuration. The deck section is rigid and symmetric with width $2D$ and vertical members of height $2H$ at the left and right ends. The masses and moments of inertia of the vertical members are neglected, and the mass of the deck is denoted M. The vertical suspension system is modeled by a spring and dashpot at each end, with spring stiffnesses K_1 and K_2 and viscous-damping coefficients C_1 and C_2 at the left and right, respectively. The effect of the rest of the deck on the section is represented by a translational spring (stiffness K_3) and dashpot (coefficient C_3), and a rotational spring (stiffness K_R) and dashpot (coefficient C_R).

From equilibrium, as shown in Fig. 1(b), the vertical deflection of the center of mass of the section is denoted $Y(T)$ and the rotation is $\theta(T)$, where T is time. In some of the examples to be presented, a vertical force $F_o \sin \Omega T$ will be assumed to act at the center of mass (e.g., representing the effect of vortices moving laterally and alternately over the top and bottom of the deck [14–16]). Like the original Tacoma Narrows Bridge, this model will exhibit vertical motion if the system is symmetric (i.e., $K_1 = K_2$ and $C_1 = C_2$) and there

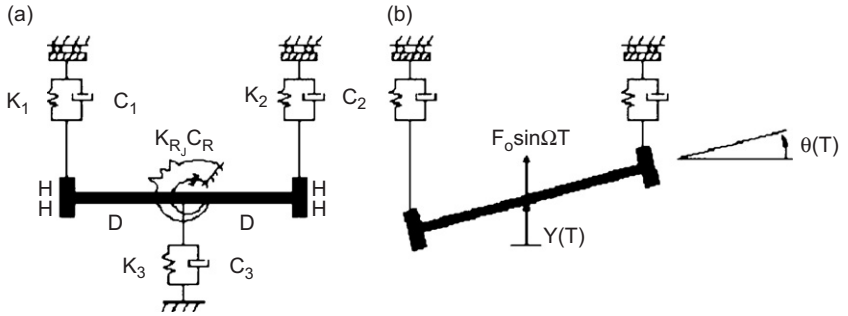

Fig. 1. Geometry of two-degree-of-freedom model: (a) in equilibrium and (b) during motion.

is no torsional excitation or disturbance, and then will demonstrate coupled vertical and torsional motion if the support conditions for the deck become asymmetric.

The coupled, nonlinear, equations of motion are given by

$$\begin{aligned} &M\ddot{Y} + C_1(\dot{Y} - D\dot{\theta}\cos\theta - H\dot{\theta}\sin\theta) + C_2(\dot{Y} + D\dot{\theta}\cos\theta - H\dot{\theta}\sin\theta) \\ &\quad + C_3\dot{Y} + K_1(Y - D\sin\theta - H\cos\theta - H) + K_2(Y + D\sin\theta + H\cos\theta - H) \\ &\quad + K_3 Y = F_o\sin\Omega T \end{aligned} \tag{1}$$

and

$$\begin{aligned} &\frac{1}{3}MD^2\ddot{\theta} - C_1\big(\dot{Y} - D\dot{\theta}\cos\theta - H\dot{\theta}\sin\theta\big)D\cos\theta \\ &\quad + C_2\big(\dot{Y} + D\dot{\theta}\cos\theta - H\dot{\theta}\sin\theta\big)D\cos\theta + C_R\dot{\theta} - K_1(Y - D\sin\theta + H\cos\theta - H)D\cos\theta \\ &\quad + K_2(Y + D\sin\theta + H\cos\theta - H)D\cos\theta + K_R\theta = 0. \end{aligned} \tag{2}$$

The analysis is conducted in terms of the following nondimensional variables:

$$\begin{aligned} &y = \frac{Y}{D}, \quad h = \frac{H}{D}, \quad t = \sqrt{\frac{g}{D}}, \quad \omega = \Omega\sqrt{\frac{D}{g}}, \quad f_o = \frac{F_o}{Mg}, \\ &k_R = \frac{K_R}{MgD}, \quad c_R = \frac{C_R}{MD\sqrt{gD}}, \quad k_j = \frac{K_j D}{Mg}, \quad c_j = \frac{C_j}{M}\sqrt{\frac{D}{g}} \\ &\qquad (j = 1, 2, 3). \end{aligned} \tag{3}$$

Then the nondimensional equations of motion are given by

$$\begin{aligned} &\ddot{y} + (c_1 + c_2 + c_3)\dot{y} + (k_1 + k_2 + k_3)y + (c_2 - c_1)\dot{\theta}\cos\theta \\ &\quad - (c_1 + c_2)h\dot{\theta}\sin\theta + (k_2 - k_1)\sin\theta + (k_1 + k_2)h(\cos\theta - 1) = f_o\sin\omega t \end{aligned} \tag{4}$$

and

$$\begin{aligned} &\frac{1}{3}\ddot{\theta} + c_R\dot{\theta} + k_R\theta + (c_1 + c_2)\dot{\theta}\cos^2\theta + (c_2 - c_1)(\dot{y} - h\dot{\theta}\sin\theta)\cos\theta \\ &\quad + (k_1 + k_2)\sin\theta\cos\theta + (k_2 - k_1)(y + h\cos\theta - h)\cos\theta = 0. \end{aligned} \tag{5}$$

If the system is symmetric and only exhibiting vertical motion, the governing equation is

$$\ddot{y} + c_o\dot{y} + k_o y = f_o\sin\omega t, \quad c_o = c_1 + c_2 + c_3, \quad k_o = k_1 + k_2 + k_3 \tag{6}$$

and its steady-state solution is

$$y(t) = \left[\left(k_o - \omega^2\right)^2 + (c_o\omega)^2\right]^{-1/2} f_o \sin(\omega t - \alpha), \tag{7}$$

where α is a constant phase.

3. Results for two-degree-of-freedom model

3.1. Sudden asymmetry in stiffness

In the first example, assume that the system exhibits steady-state motion as in Eq. (7), with $\theta = 0$ until $t = 0$. The parameters for $t<0$ are $h = 0.12$, $f_o = 1$, $\omega = 2$, $k_1 = k_2 = 0.4$, $k_3 = k_R = c_1 = c_2 = 0.01$, and $c_R = c_3/3$. At $t = 0$, a sudden asymmetric change is assumed to occur in the support conditions: the stiffness coefficient k_2 for the right suspension drops from 0.4 to 0.35. The time histories are shown in Fig. 2 for $-10<t<50$, with $y(t)$ plotted in Fig. 2(a) and $\theta(t)$, in Fig. 2(b). For $t<0$, y is harmonic with nondimensional period π. Numerical results in this study were obtained using Mathematica [17].

In this example, the change of stiffness on one side of the section does not have a significant effect on the magnitude of the vertical motion, although y appears to change into a period-2 motion with slightly different amplitudes at adjacent peaks. Torsional motion is induced at $t = 0$. The rotational angle θ seems to exhibit almost a period-4 motion, but with small decay.

If damping and the applied force are not included, and if Eqs. (4) and (5) are linearized, the nondimensional natural frequencies for the parameters used when $t<0$ are 0.894 (corresponding to vertical motion with no rotation, i.e., $\theta = 0$) and 1.549 (corresponding to rotational motion about the center of mass of the bar, i.e., $y = 0$). For the parameters used when $t>0$, the natural frequencies are 0.863 (with $y = 10.0\theta$) and 1.502 (with $\theta = -30.0y$). Hence the excitation frequency used in Fig. 2 is higher than the two natural frequencies for small, free vibrations about equilibrium.

3.2. Sudden asymmetry in damping

As a second example, the parameters for $t<0$ are the same as before except that $\omega = 1.55$. At $t = 0$, the damping coefficient c_2 on the right suspension suddenly jumps from 0 to 0.1. Results are plotted in Fig. 3, again for $-10<t<50$. The period for the vertical motion is 4.05 for $t<0$. After the damping of the system becomes asymmetric, $y(t)$ demonstrates some transient motion, and $\theta(t)$ grows and then exhibits harmonic motion with the period 4.05 of the excitation. This example includes a feature of the behavior of the original Tacoma Narrows Bridge, in that sudden slipping of the suspension cable through a band on one side of the deck caused an asymmetrical friction condition and led to steady-state vertical–torsional oscillations.

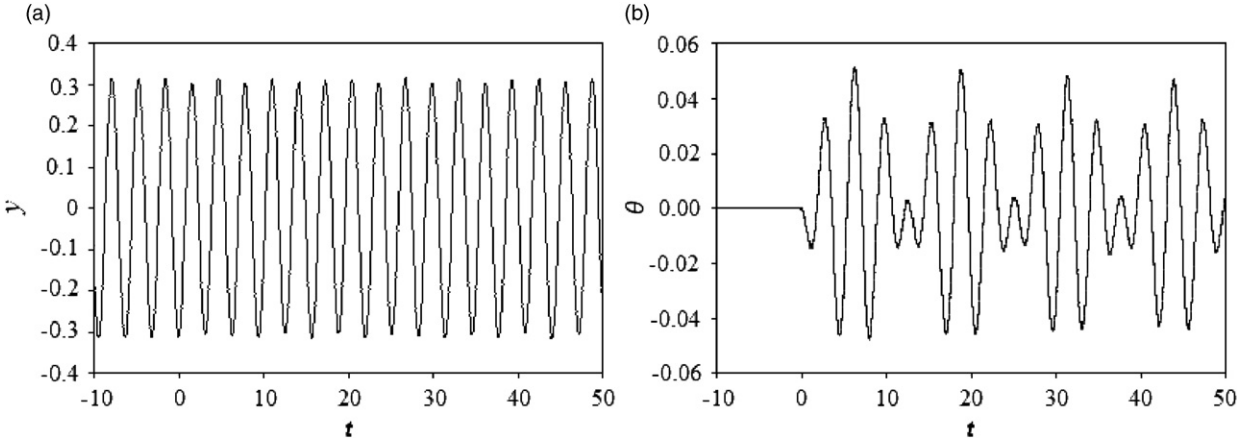

Fig. 2. Time histories for two-degree-of-freedom model with sudden decrease of k_2 at $t = 0$: (a) vertical motion and (b) rotational motion.

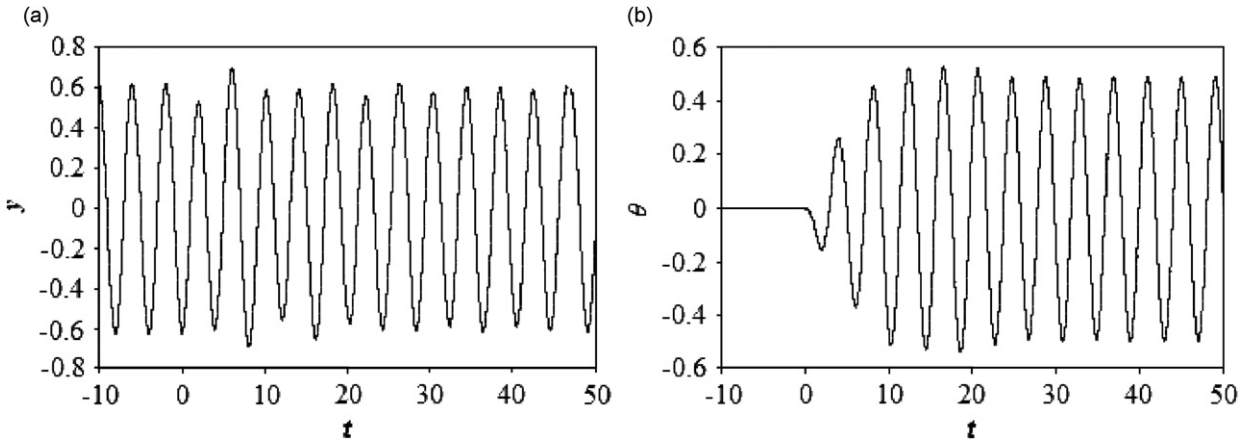

Fig. 3. Time histories for two-degree-of-freedom model with sudden increase of c_2 at $t = 0$: (a) vertical motion and (b) rotational motion.

3.3. Aerodynamic moment

The previous examples have not considered an applied moment on the deck, which may be caused by vortex shedding (due to the resultant lift vector acting eccentrically to the center of mass) or by other excitations. For a given wind speed, wind direction, and oscillation frequency of the deck, aerodynamic forces on bridge decks are often assumed to be linear functions of the deck's vertical, lateral, and torsional displacements and velocities [18]. With regard to torsional oscillations, the most important term in these linear relations seems to be the dependence of the torsional (pitching) moment on the torsional velocity. For sufficiently high wind speeds, this term acts like a "negative damping" and feeds energy into the deck, and the torsional motion tends to grow until stiffening effects of the system may limit the growth and cause a steady-state motion (limit cycle) to occur [19].

First assume that no nonlinearities are present, and that the difference of the aerodynamic moment and the resisting rotational viscous damping (called "aerodynamic torsional damping" and "mechanical torsional damping," respectively, in Ref. [15]) leads to an effective negative damping coefficient $c_R = -0.0045$. The other parameters are chosen to be $h = 0.12$, $f_o = 0$, $k_1 = 0.4$, $k_2 = 0.35$, $k_3 = k_R = c_1 = c_2 = 0$, and $c_3 = 0.01$. With arbitrary c_R, the Routh–Hurwitz conditions applied to the linearized equations of motion show that the equilibrium state is unstable if $c_R < -1.10 \times 10^{-5}$, which is the case for this example. The motion is assumed to begin at $t = 0$ with small initial conditions. Time histories are plotted for $0 < t < 3{,}000$ in Fig. 4. After some decrease of the vertical motion from $y(0) = 0.01$, both displacements increase steadily and grow unboundedly.

3.4. Nonlinear damping

The original Tacoma Narrows Bridge exhibited a limit cycle for about an hour before collapse occurred. One simple, nonlinear, mathematical model that induces a limit cycle is the van der Pol type of damping, which is negative for small amplitudes of motion and then positive for large amplitudes. Such a model was considered in Refs. [14,15,20] for vertical wind-induced oscillations of a bridge deck. Here such a term is included in Eq. (5) for torsional motion. The second term, with negative coefficient c_R, is now multiplied by $(1-\eta\theta^2)$, where η is a positive constant.

Fig. 5 shows the time histories of y and θ for the following set of parameters: $h = 0.12$, $f_o = 0$, $k_1 = 0.4$, $k_2 = 0.35$, $k_3 = k_R = 0$, $c_1 = c_2 = c_3 = 0.01$, $c_R = -0.0045$, and $\eta = 0.5$. In the initial conditions, y and θ are chosen to be 0.01, and the initial velocities are zero. The response to the aerodynamic moment, which is in the unstable range, is small in the vertical deflection for a while, as the rotation grows steadily. Then both displacements grow and approach a limit cycle with large amplitudes. The nondimensional frequency of oscillations in the limit cycle is 0.88, which is slightly higher than the fundamental natural frequency of 0.863

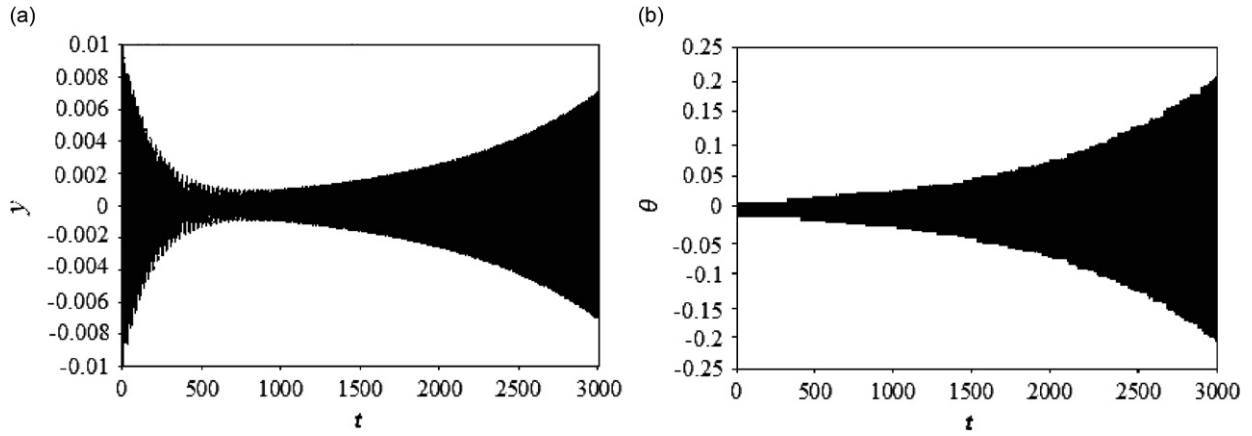

Fig. 4. Time histories for two-degree-of-freedom model with high aerodynamic moment: (a) vertical motion and (b) rotational motion.

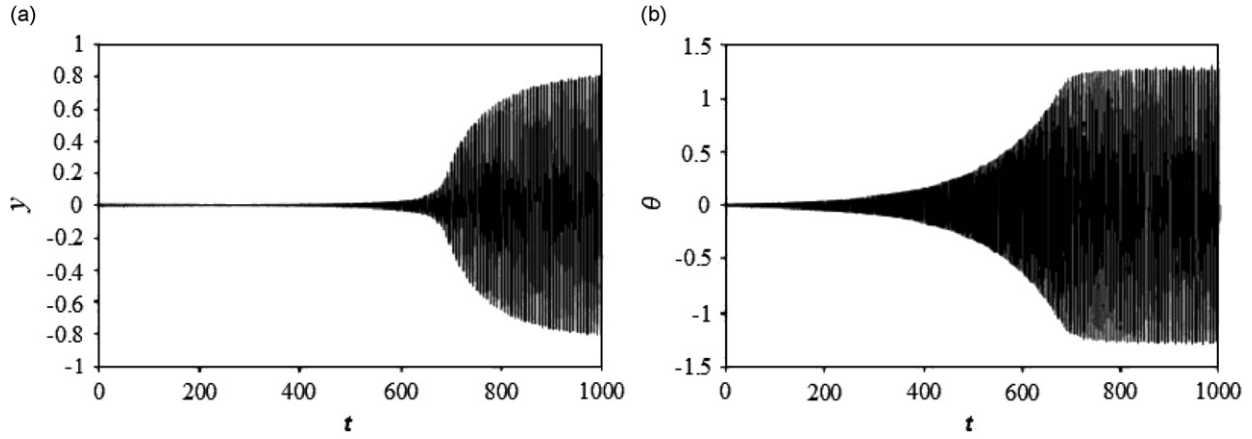

Fig. 5. Time histories for two-degree-of-freedom model with high aerodynamic moment and van der Pol nonlinear damping: (a) vertical motion and (b) rotational motion.

for small vibrations. The motion does not resemble that of either the first or second vibration mode, since y and θ have similar amplitudes in the limit cycle.

3.5. Nonlinear hanger force

Under aerodynamic conditions that lead to torsional flutter, a limit cycle also could be caused by nonlinear (stiffening) forces in the hangers. Here such forces are assumed to be cubic functions of the elongation. The terms $k_8(y+\sin\theta+h\cos\theta-h)^3+k_7(y-\sin\theta-h\cos\theta-h)^3$ are now included in the left-hand side of Eq. (4), and the terms $k_8(y+\sin\theta+h\cos\theta-h)^3\cos\theta-k_8(y-\sin\theta-h\cos\theta-h)^3\cos\theta$ are added to the left-hand side of Eq. (5), where k_7 and k_8 are positive coefficients.

Results are depicted in Fig. 6 for $h=0.12$, $f_o=0$, $k_1=0.4$, $k_2=0.35$, $k_3=k_R=0$, $c_1=c_2=c_3=0.01$, $c_R=-0.021$, and the coefficients $k_7=k_8=100$ for the nonlinear force components of the hangers. With the new (nonzero) values of c_2 and c_3 in this example, the critical value of c_R is -0.020, so the system is barely unstable. The initial conditions are zero except for $y(0)=0.5$. As for the example with nonlinear damping in Fig. 5, here the motion also approaches a limit cycle involving the vertical displacement and rotational motion.

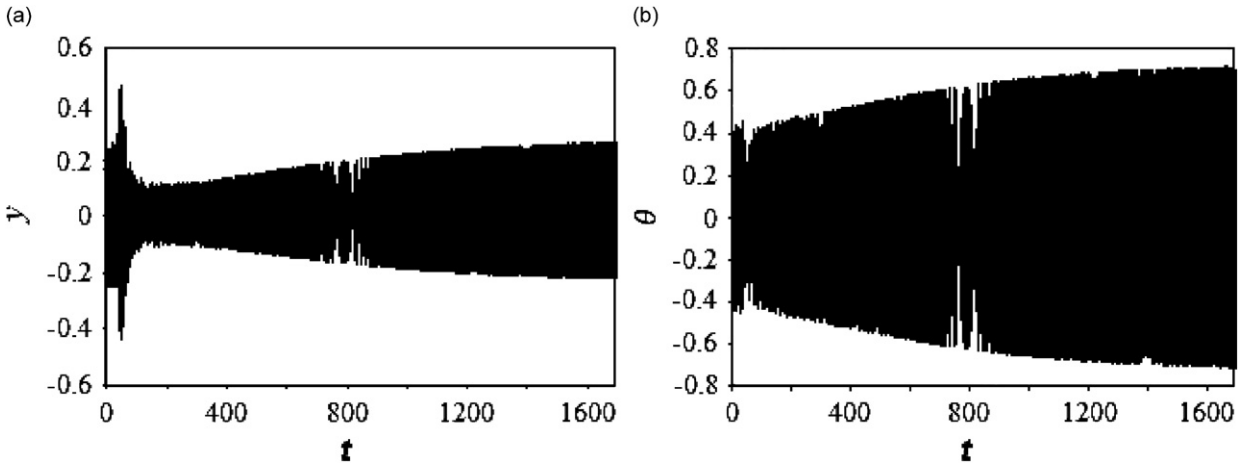

Fig. 6. Time histories for two-degree-of-freedom model with high aerodynamic moment and nonlinear hanger force: (a) vertical motion and (b) rotational motion.

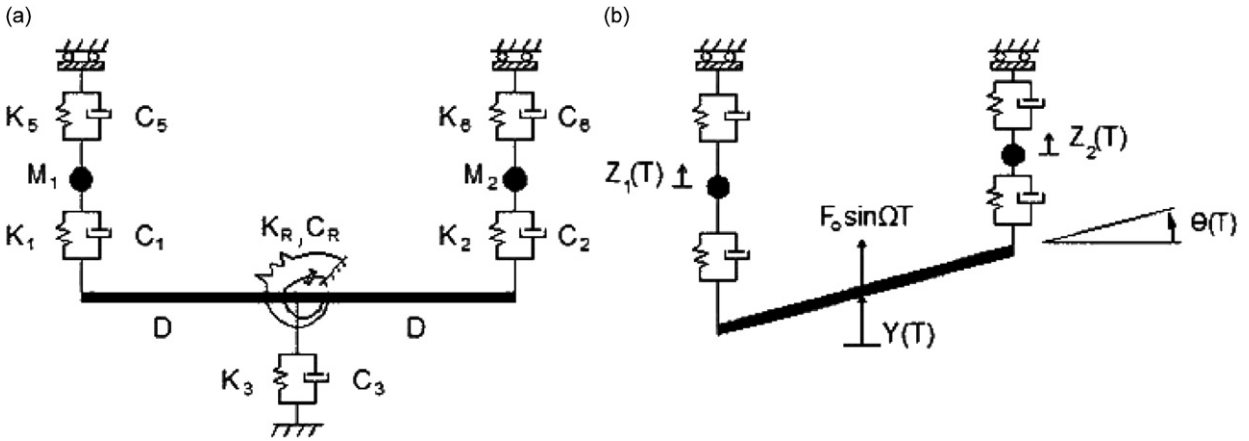

Fig. 7. Geometry of four-degree-of-freedom model: (a) in equilibrium and (b) during motion.

4. Formulation for four-degree-of-freedom model

The four-degree-of-freedom model is depicted in Fig. 7. The results for the two-degree-of-freedom model turned out to be almost the same if $h = H/D = 0.12$, as used, or $h = 0$. For simplicity, $h = 0$ in this section. The bottom part of the model is the same as in Fig. 1 (but with $H = 0$). The suspension cables are represented by point masses M_1 and M_2, vertical springs with stiffnesses K_5 and K_6, and vertical dashpots with damping coefficients C_5 and C_6, as shown in Fig. 2(a). The vertical displacements of the cable masses from equilibrium are denoted $Z_1(T)$ and $Z_2(T)$, as shown in Fig. 2(b).

The nondimensional variables in Eqs. (3) are used, along with $z_j = Z_j/D$ and $m_j = M_j/M$ for $j = 1,2$, and $k_j = K_jD/(Mg)$ for $j = 5,6$. In nondimensional form, the four equations of motion are:

$$\ddot{y} + c_o\dot{y} + k_o y + (c_2 - c_1)\dot{\theta}\cos\theta + (k_2 - k_1)\sin\theta - c_1\dot{z}_1 - c_2\dot{z}_2 - k_1 z_1 - k_2 z_2 = f_o \sin\omega t, \tag{8}$$

$$\frac{1}{3}\ddot{\theta} + c_R\dot{\theta} + k_R\theta + (c_1 + c_2)\dot{\theta}\cos^2\theta + (k_1 + k_2)\sin\theta\cos\theta + (c_2 - c_1)\dot{y}\cos\theta + (k_2 - k_1)y\sin\theta + (c_1\dot{z}_1 - c_2\dot{z}_2)\cos\theta + (k_1 z_1 - k_2 z_2)\cos\theta = 0, \tag{9}$$

$$m_1\ddot{z}_1 + (c_1 + c_5)\dot{z}_1 + (k_1 + k_5)z_1 - c_1\left(\dot{y} - \dot{\theta}\cos\theta\right) - k_1(y - \sin\theta) = 0 \tag{10}$$

and

$$m_2\ddot{z}_2 + (c_2 + c_6)\dot{z}_2 + (k_2 + k_6)z_2 - c_2\left(\dot{y} + \dot{\theta}\cos\theta\right) - k_2(y + \sin\theta) = 0. \tag{11}$$

5. Results for four-degree-of-freedom model

5.1. Sudden asymmetry in stiffness

As in Section 3.1 and Fig. 2, it is assumed that the system exhibits steady-state vertical vibrations and then experiences a sudden change in k_2, the stiffness of a hanger (suspender) connecting one edge of the deck to the suspension cable above it. Here, the parameters for $t<0$ are $f_o = 1$, $m_1 = m_2 = 0.17$, $k_1 = k_2 = 0.4$, $k_3 = k_R = 0$, $k_5 = 0.3$, $k_6 = 0.3$, $c_1 = c_2 = 0$, $c_3 = 0.01$, $c_R = c_3/3$, and $c_5 = c_6 = 0.0025$. At $t = 0$, the stiffness coefficient k_2 again suddenly decreases to 0.35. Time histories for the four coordinates are depicted in Fig. 8 for $-10 < t < 50$. In this case, the sudden introduction of a lateral asymmetry in the supporting stiffness of the deck has little effect on the vertical displacements of the suspension cables and the center of mass of the deck (which exhibit period-1 motion), but induces torsional oscillations, as expected.

If undamped, unforced, small vibrations about equilibrium are considered, the nondimensional natural frequencies for the parameters when $t<0$ are 0.553, 0.856, 2.147, and 2.405. The first and third modes are symmetric (i.e., $\theta = 0$), whereas $y = 0$ for the second and fourth modes. In the first mode, $z_1 = z_2 = 0.617y$. In the second mode, $z_1 = -z_2 = -0.695\theta$. In the third mode, $z_1 = z_2 = -4.76y$. In the fourth mode, $z_1 = -z_2 = 1.41\theta$. For the parameters used when $t>0$, the natural frequencies are 0.547, 0.850, 2.091, and 2.355 (slightly lower than for $t<0$), and all four modes involve y and θ since the system is asymmetric. The ratios y/θ for the first four modes, respectively, are 25.00, −0.0107, 1.770, and −0.0780.

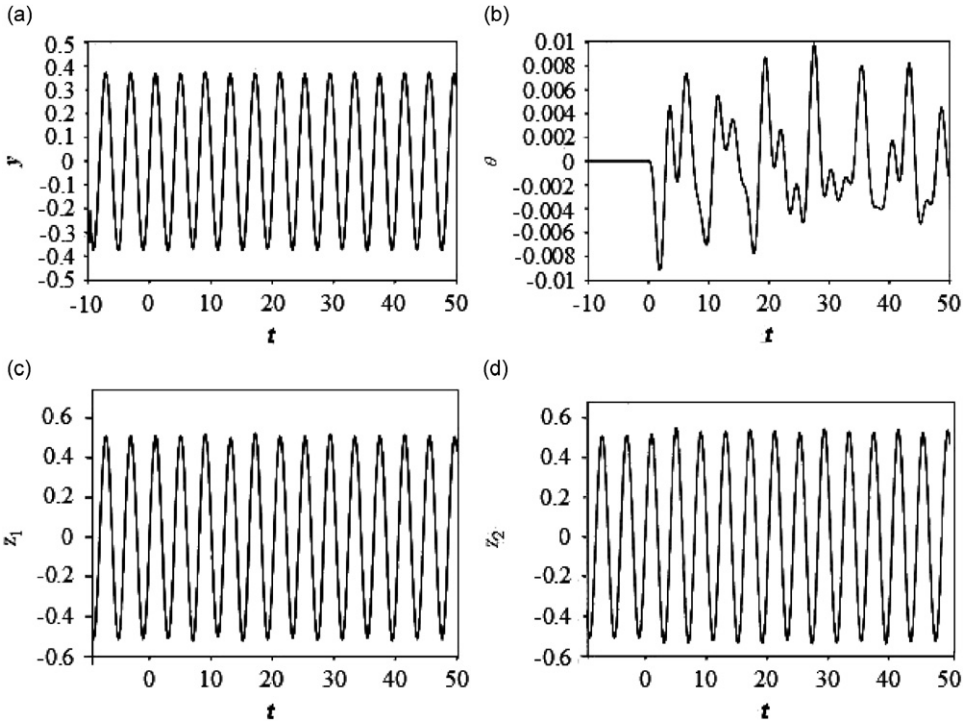

Fig. 8. Time histories for four-degree-of-freedom model with sudden decrease of k_2 at $t = 0$: (a) vertical motion of deck; (b) rotational motion of deck; (c) vertical motion of M_1; and (d) vertical motion of M_2.

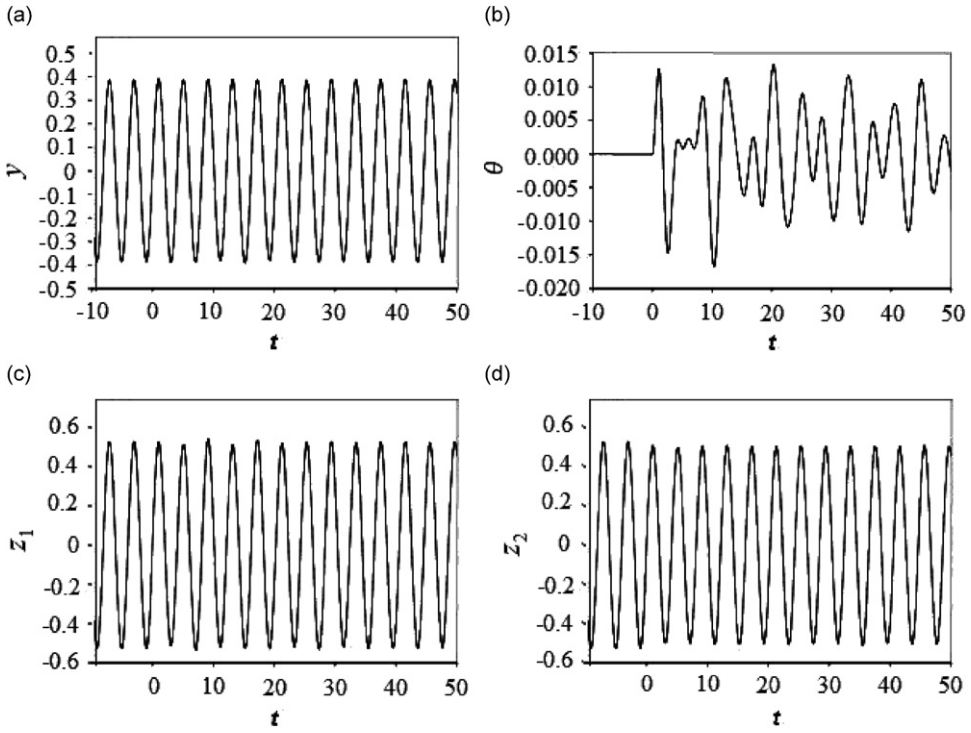

Fig. 9. Time histories for four-degree-of-freedom model with sudden increase of c_2 at $t = 0$: (a) vertical motion of deck; (b) rotational motion of deck; (c) vertical motion of M_1; and (d) vertical motion of M_2.

5.2. Sudden asymmetry in damping

As for the two-degree-of-freedom example in Section 3.2, now k_2 does not change, but the damping coefficient c_2 is suddenly increased from 0 to 0.1 at $t = 0$. The parameters are the same as in Section 5.1 except that $k_3 = k_R = 0.1$. The results shown in Fig. 9 for this case are similar to those in Fig. 8.

In this case, the nondimensional natural frequencies are 0.628, 0.964, 2.150, and 2.427. The symmetry properties are the same as in Section 5.1. In the first mode, $z_1 = z_2 = 0.632y$. In the second mode, $z_1 = -z_2 = -0.738\theta$. In the third mode, $z_1 = z_2 = -4.65y$. In the fourth mode, $z_1 = -z_2 = 1.33\theta$.

5.3. Aerodynamic moment

Similarly to Section 3.3, now the wind speed is assumed to be greater than the critical speed for torsional oscillations. The parameters used to obtain the results in Fig. 10 are $f_o = 1$, $\omega = 1.55$, $m_1 = m_2 = 0.17$, $k_1 = 0.4$, $k_2 = 0.35$, $k_3 = k_R = 0.1$, $k_5 = k_6 = 0.3$, $c_1 = c_2 = 0$, $c_3 = 0.01$, $c_R = -0.006$, and $c_5 = c_6 = 0.0025$. The initial conditions are $y = \theta = z_1 = z_2 = 0.01$ with no initial velocities. The vertical displacements of the cables and the center of mass of the deck seem to settle into limit cycles, whereas the torsional oscillations grow and become large. (If f_o were set equal to zero, all the variables would grow.) For the values of m_1, m_2, k_1, k_2, k_3, k_R, k_5, and k_6 used in this example, the natural frequencies are 0.623, 0.960, 2.095, and 2.376. The modes involve y and θ. The ratios y/θ for the first four modes are 34.94, −0.0063, 1.838, and −0.0717, respectively. The magnitudes of z_1 and z_2 are smaller than the magnitude of y in the first mode and larger in the other three modes.

5.4. Nonlinear hanger force

Similarly to the case treated in Section 3.5, the forces in the hangers connected to the edges of the deck are assumed to have cubic stiffening components. The terms added to the left-hand sides of Eqs. (8)–(11),

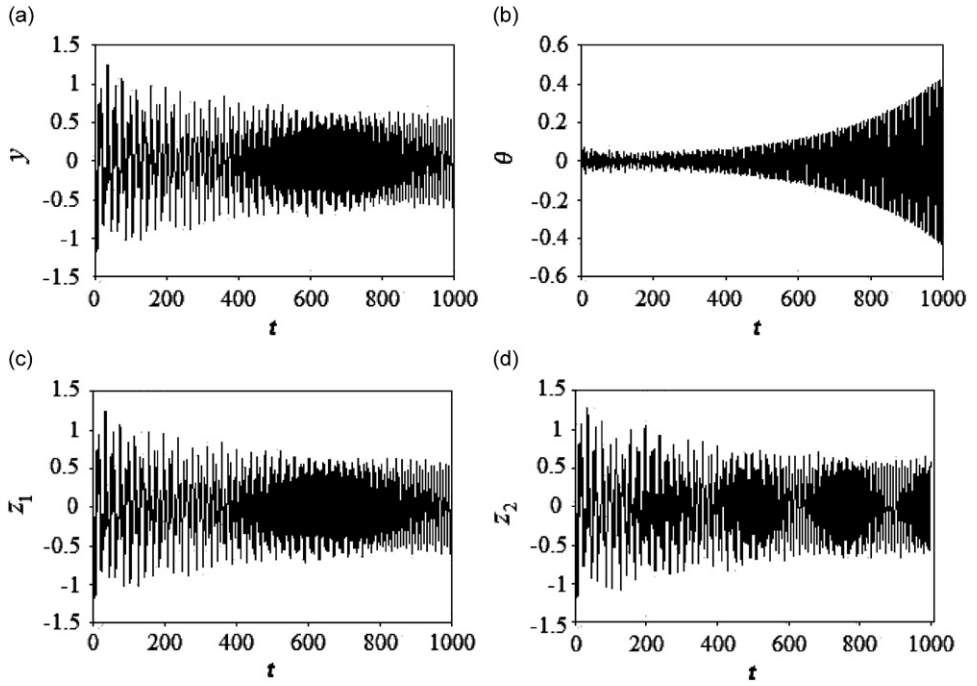

Fig. 10. Time histories for four-degree-of-freedom model with high aerodynamic moment: (a) vertical motion of deck; (b) rotational motion of deck; (c) vertical motion of M_1; and (d) vertical motion of M_2.

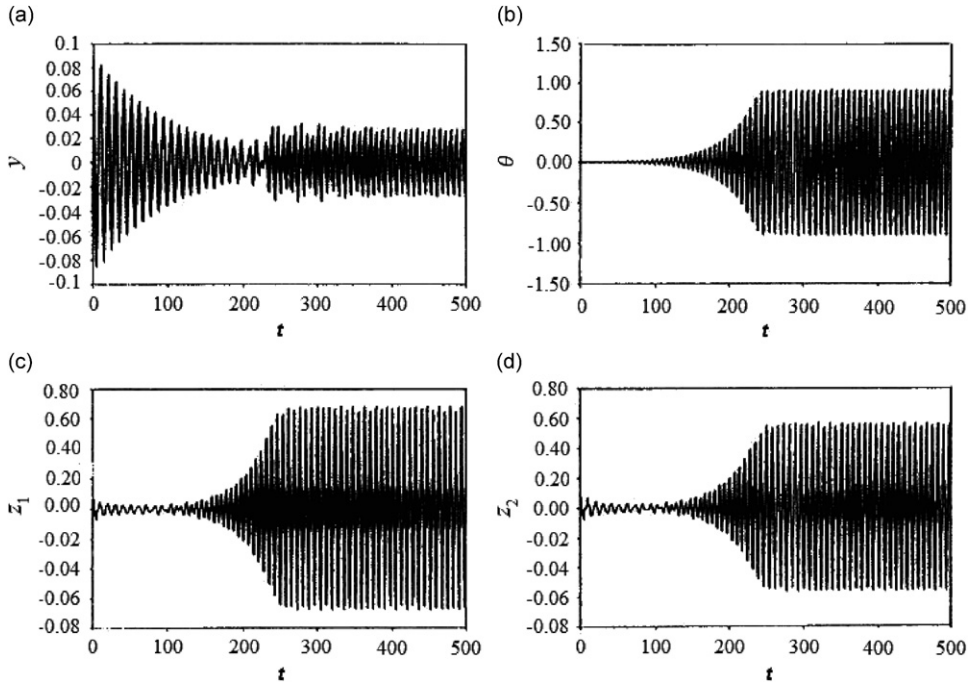

Fig. 11. Time histories for four-degree-of-freedom model with high aerodynamic moment and nonlinear hanger force: (a) vertical motion of deck; (b) rotational motion of deck; (c) vertical motion of M_1; and (d) vertical motion of M_2.

respectively, are (i) $k_8(y+\sin\theta-z_2)^3+k_7(y-\sin\theta-z_1)^3$; (ii) $k_8(y+\sin\theta-z_2)^3\cos\theta-k_7(y-\sin\theta-z_1)^3\cos\theta$; (iii) $-k_7(y-\sin\theta-z_1)^3$; and (iv) $-k_8(y+\sin\theta-z_2)^3$. Results are presented in Fig. 11 for the case $f_o=0$, $m_1=m_2=0.17$, $k_1=0.4$, $k_2=0.35$, $k_3=k_R=0.1$, $k_5=k_6=0.4$, $c_1=c_2=0.02$, $c_3=0.01$,

$c_R = -0.004$, and $c_5 = c_6 = 0.0025$, and small cubic coefficients $k_7 = k_8 = 0.001$. First the vertical deflection y decays from its initial value of 0.1 and the other displacements remain small. Then all displacements increase and enter into a limit cycle with significant rotation of the deck and asymmetric vertical motions of the cables (since the linear components of the hanger forces are asymmetric).

For the case in Fig. 11, the natural frequencies for small vibrations are 0.668, 1.054, 2.217, and 2.459. The ratios y/θ for the first four modes, respectively, are 27.73, −0.0088, 1.645, and −0.0767. The frequency of the limit-cycle motion is 0.80, which is between the first and second natural frequencies.

6. Concluding remarks

If a suspension bridge or cable-stayed bridge is symmetric with respect to its centerline, and if the external excitation is small (such as light traffic or light wind), the deck should exhibit very little torsional motion. Most decks are torsionally stiff. The original Tacoma Narrows Bridge was not. However, it did not exhibit noticeable torsional oscillations, even under high winds, until a sudden lateral asymmetry occurred. The midspan cable band on the north side loosened, allowing the north suspension cable to slip back and forth through the band, which facilitated torsional motion of the deck. A sudden lateral asymmetry also could be produced by the loss of one or more cables in a cable-stayed bridge or hangers in a suspension bridge, e.g., due to accident, fatigue, earthquake, fire, or intentional act.

Obviously, an asymmetrical condition with respect to the centerline will induce torsional motion. This paper has presented some quantitative results in the form of transient time histories of the vertical and rotational responses of a cross section of a deck, along with vertical cable motions (at that section) in some cases. The results demonstrate how the torsional motion may grow, and in some cases reach a limit cycle with small or large amplitude. Previous analyses of straight bridges under wind loads (including the original Tacoma Narrows Bridge) have typically assumed symmetry of the structure about the centerline.

For the two-degree-of-freedom case, the deck was modeled as an *H*-section, the shape that has been used to represent the deck of the original Tacoma Narrows Bridge. For the four-degree-of-freedom case, the deck was represented as a rigid bar. Translational springs and dashpots were used to represent the hangers, and other resistance (e.g., from the rest of the deck) was modeled by additional translational and rotational springs and dashpots. Numerical values of parameters and initial conditions were chosen to demonstrate typical types of response, and were not related to dimensional values from any particular bridge.

The governing equations for the two-degree-of-freedom and four-degree-of-freedom section models include geometric nonlinearities. If the wind speed is sufficiently high to cause torsional flutter, other nonlinearities may be needed to keep the numerical response bounded (as occurs in real structures). Both nonlinear damping (of the van der Pol type) and nonlinear forces in the hangers (cubic stiffening) were included in some examples, and then the oscillations approached a limit cycle, with approximately constant amplitudes of the translational and rotational motions (as exhibited in the original Tacoma Narrows Bridge for about 1 h prior to its collapse). The behavior would not change significantly if slight changes were made in the initial conditions.

Small, free vibrations of the section models also were analyzed, and in some cases the frequency of the limit cycle turned out to lie between the first and second natural frequencies of the system. In the examples, the springs remained in tension, so that the nonlinearity associated with cable slackness [3] was not encountered, nor were snap loads that may occur when slack cables become taut.

Acknowledgements

This material is based upon work supported by the US National Science Foundation under Grant no. 0114709. The authors are grateful to Richard Scott and Richard S. Hobbs for information and considerable assistance regarding the original Tacoma Narrows Bridge. The authors also thank the reviewers for their helpful comments.

References

[1] R. Scott, *In the Wake of Tacoma*, American Society of Civil Engineers, Reston, VA, 2001.
[2] Y. Rocard, *Dynamic Instability*, Crosby Lockwood and Son, London, 1957.

[3] A.C. Lazer, P.J. McKenna, Large-amplitude periodic oscillations in suspension bridges: some new connections with nonlinear analysis, *SIAM Review* 32 (1990) 537–578.
[4] K.Y. Billah, R.H. Scanlan, Resonance, Tacoma Narrows Bridge failure, and undergraduate physics textbooks, *American Journal of Physics* 59 (1991) 118–124.
[5] H. Petroski, Still twisting, *American Scientist* 79 (1991) 398–401.
[6] D. Berreby, The great bridge controversy, *Discover* February (1992) 26–33.
[7] D. Jacover, P.J. McKenna, Nonlinear torsional flexings in a periodically forced suspended beam, *Journal of Computational and Applied Mathematics* 52 (1994) 241–265.
[8] P.J. McKenna, Large torsional oscillations in suspension bridges revisited: fixing an old approximation, *American Mathematical Monthly* 106 (1999) 1–18.
[9] S.H. Doole, S.J. Hogan, Non-linear dynamics of the extended Lazer–McKenna bridge oscillation model, *Dynamics and Stability of Systems* 15 (2000) 43–58.
[10] P.J. McKenna, C. Ó Tuama, Large torsional oscillations in suspension bridges visited again: vertical forcing creates torsional response, *American Mathematical Monthly* 108 (2001) 738–745.
[11] P.J. McKenna, K.S. Moore, The global structure of periodic solutions to a suspension bridge mechanical model, *IMA Journal of Applied Mathematics* 67 (2002) 459–478.
[12] V. Sepe, G. Augusti, A deformable section model for the dynamics of suspension bridges, part I: model and linear response, *Wind and Structures* 4 (2001) 1–18.
[13] V. Sepe, M. Diaferio, G. Augusti, A "deformable section" model for the dynamics of suspension bridges, part II: nonlinear analysis and large amplitude oscillations, *Wind and Structures* 6 (2003) 451–470.
[14] F. Ehsan, R.H. Scanlan, Vortex-induced vibrations of flexible bridges, *Journal of Engineering Mechanics* 116 (1990) 1392–1411.
[15] R.H. Scanlan, Bridge flutter derivatives at vortex lock-in, *Journal of Structural Engineering* 124 (1998) 450–458.
[16] A. Larsen, Aerodynamics of the Tacoma Narrows Bridge—60 years later, *Structural Engineering International* 4 (2000) 243–248.
[17] S. Wolfram, *The Mathematica Book*, third ed., Cambridge University Press, Cambridge, UK, 1996.
[18] E. Simiu, T. Miyata, *Design of Buildings and Bridges for Wind: a Practical Guide for ASCE-7 Standard Users and Designers*, Wiley, Hoboken, NJ, 2006.
[19] R.H. Scanlan, J.J. Tomko, Airfoil and bridge deck flutter derivatives, *Journal of the Engineering Mechanics Division, American Society of Civil Engineers* 97 (1971) 1717–1737.
[20] H. Gupta, P.P. Sarkar, K.C. Mehta, Identification of vortex-induced-response parameters in time domain, *Journal of Engineering Mechanics* 122 (1996) 1031–1037.